MATIMYÁS MATEMATIKA
ISSN 0115-6926

Journal of the Mathematical Society of the Philippines
Vol. 49 No. 1 (2026) pp. 13-34

Criticality of Hopf Bifurcations and Quasi-Periodic Oscillations in a Stage Structured Intraguild Predation Model

Anthony M. Pasion[1,2] and Juancho A. Collera[2]

[1]Department of Mathematics and Statistics
Queen's University
Kingston, Ontario K7L 3N6 Canada
anthony.pasion@queensu.ca

[2]Department of Mathematics and Computer Science
University of the Philippines Baguio
Baguio City 2600, Philippines
jacollera@up.edu.ph

Abstract

Previously, a three-species intraguild (IG) predation model wherein the IG prey population is partitioned into juvenile and adult stages has been proposed. This model was described using a system of delay differential equations with delay-dependent coefficients in which the time delay represents the age of maturation in the IG prey population. It was shown that Hopf bifurcations occur in this system when the time-delay parameter is varied. This gives rise to limit-cycle solutions, which provide scenarios for periodic coexistence between species. In this paper, we determine the criticality of these Hopf bifurcations, as well as the stability of the bifurcating branch of limit cycles from these Hopf bifurcations. Our main tool is the centre manifold reduction and normal form theory due to Hassard, Kazarinoff and Wan. We then illustrate the results using numerical continuation. Furthermore, our simulations show that the stability along a branch of period-one limit cycles may switch due to the presence of torus bifurcations. This justifies the observed quasi-periodic oscillations for certain values of the time-delay parameter when neither the coexistence equilibrium nor the period-one cycle is stable.

Keywords: Hopf bifurcation, centre manifold reduction, intraguild predation, quasi-periodic oscillations, numerical continuation

2020 MSC: 34K17, 37G15, 92D40

1 Preliminaries

In [6], Collera and Magpantay studied a three-species intraguild (IG) predation model composed of the basal resource, the IG prey, and the IG predator. The IG prey population is further subdivided into immature and mature stages, and under the assumption that the immature IG preys have little ability of predation and are able to avoid predation by taking refuge. Their model is the following system of delay differential equations (DDEs) with delay-dependent coefficients

$$\begin{cases} \dot{x}(t) &= x(t)\ \big[a_0 - a_1 x(t) - a_2 y(t) - a_3 z(t)\big], \\ \dot{y}(t) &= y(t)\ \big[-b_0 - b_3 z(t)\big] + b_1 e^{-\mu\tau} x(t-\tau) y(t-\tau)\ , \\ \dot{z}(t) &= z(t)\ \big[-c_0 + c_1 x(t) + c_2 y(t)\big], \end{cases} \tag{1}$$

where the state variables $x(t)$, $y(t)$ and $z(t)$ denote the population at time t of the basal resource, the mature IG prey and the IG predator, respectively. The parameter $\mu > 0$ is the death rate of the immature IG preys, while the time-delay parameter $\tau > 0$ is the age of maturation in the IG prey population. Thus, the term $b_1 e^{-\mu\tau} x(t-\tau) y(t-\tau)$ in the second equation of the system (1) represents the number of immature IG preys that were born at the previous time $(t - \tau)$ and still survives to the present time t and hence, are transferred from the immature stage to the mature stage at time t. We refer the readers to [6] for the diagram of the interactions between the species and the details of the derivation of the system (1), as well as the description of the rest of the system parameters. The readers may also refer to the seminal work of Holt and Polis [15] on the theoretical framework for IG predation. Meanwhile, the works of Wang et al. [18] and Yamaguchi et al. [19] provide the mathematical background on stage structured populations.

The positive equilibrium of the system (1), as derived in [6] and referred to as the *coexistence equilibrium*, is given by

$$E_* = (x_*, y_*, z_*)\ , \tag{2}$$

where the positive components are as follows:

$$\begin{aligned} x_* &= \frac{a_0 b_3 c_2 - a_2 b_3 c_0 + a_3 b_0 c_2}{a_1 b_3 c_2 - a_2 b_3 c_1 + a_3 b_1 c_2 e^{-\mu\tau}}, \\ y_* &= \frac{-a_0 b_3 c_1 + a_1 b_3 c_0 - a_3 b_0 c_1 + a_3 b_1 c_0 e^{-\mu\tau}}{a_1 b_3 c_2 - a_2 b_3 c_1 + a_3 b_1 c_2 e^{-\mu\tau}}, \\ z_* &= \frac{(a_0 c_2 - a_2 c_0) b_1 e^{-\mu\tau} - a_1 b_0 c_2 + a_2 b_0 c_1}{a_1 b_3 c_2 - a_2 b_3 c_1 + a_3 b_1 c_2 e^{-\mu\tau}}. \end{aligned}$$

The dynamics near the coexistence equilibrium E_* was examined by analyzing the distribution of the roots of the following characteristic equation, which corresponds to the linearized system around the coexistence equilibrium E_*:

$$\det\left(\lambda I - \begin{bmatrix} s_1 & s_2 & s_3 \\ 0 & s_4 & s_5 \\ s_6 & s_7 & 0 \end{bmatrix} - \begin{bmatrix} 0 & 0 & 0 \\ b_1 e^{-\mu\tau} y_* & b_1 e^{-\mu\tau} x_* & 0 \\ 0 & 0 & 0 \end{bmatrix} e^{-\lambda\tau}\right) = 0, \tag{3}$$

where the matrix entries are given by

$$s_1 = -a_1 x_*, \tag{4}$$
$$s_2 = -a_2 x_*, \tag{5}$$
$$s_3 = -a_3 x_*, \tag{6}$$
$$s_4 = -b_0 - b_3 z_*, \tag{7}$$
$$s_5 = -b_3 y_*, \tag{8}$$
$$s_6 = c_1 z_*, \tag{9}$$
$$s_7 = c_2 z_*. \tag{10}$$

The characteristic equation (3) is a transcendental equation with delay-dependent coefficients since all the matrix entries are in terms of the components x_*, y_* and z_* which in turn depend on the time-delay parameter τ.

The behaviour or dynamics of a system may change when a parameter is varied. This transition from one state to another is referred to as a *bifurcation*. For systems of DDEs, varying the time-delay parameter may give rise to the so-called *Hopf bifurcations* which indicate the birth (or death) of a periodic orbit around an equilibrium. The theory developed by Beretta and Kuang [3] on DDEs with delay-dependent parameters was used to derive the conditions for the Hopf bifurcation to occur around the coexistence equilibrium E_*. In particular, it was shown that the system (1) undergoes a Hopf bifurcation at E_* at some critical values of the time-delay parameter [6, Theorem 5]. Moreover, these Hopf bifurcations induce stability switches. Thus, studying the nature of these Hopf bifurcations is indispensable in the understanding of species coexistence.

In the following section, we further examine these Hopf bifurcations by looking at their direction and the stability of the bifurcating limit-cycle solutions. The main tool here is the centre manifold reduction followed by the normal form method formulated by Hassard et al. [14], which applies to the system (1). We then illustrate the main results using numerical continuation in order to visualize the branches of limit cycles emanating from the Hopf bifurcations. Coincidentally, the numerical simulation led to the discovery of quasi-periodic oscillations attributed to the presence of torus bifurcations. We end with a summary and conclusions of the paper.

2 Main Results

From this point on, we assume that the system (1) undergoes a Hopf bifurcation around the coexistence equilibrium E_* when the maturation age $\tau = \tau^*$, and denote by $\pm i\omega$ the corresponding conjugate pair of purely imaginary roots of the characteristic equation (3), that is, $\lambda(\tau^*) = \pm i\omega$. Moreover, at $\tau = \tau^*$, we assume that all other roots of the characteristic equation (3) lie inside the open left-half of the complex plane and that the roots on the imaginary axis $\lambda(\tau^*) = \pm i\omega$ are simple.

The analysis in this section follows the classical framework of Hassard et al. [14] for Hopf bifurcation in delay differential equations. Since delay differential equations are naturally infinite-dimensional dynamical systems, the first step is to rewrite the original model as an abstract differential equation on an appropriate phase space. One then reduces the local dynamics near the Hopf bifurcation point to a finite-dimensional centre manifold. This reduction is one of the fundamental uses of centre manifold theory in infinite-dimensional systems. It allows the original problem to be replaced locally by an ordinary differential equation on a low-dimensional invariant manifold tangent to the centre subspace near a non-hyperbolic equilibrium. In the setting of delay equations, this is especially useful because it converts the local analysis into the more familiar finite-dimensional framework (see, for instance, [2, 7], and the references therein). Once the reduced system has been obtained, normal form theory is then used to simplify its nonlinear terms and isolate the coefficients that govern the local bifurcation behaviour. In particular, the normal form method transforms the reduced system into one with a simpler analytic expression but with the same local qualitative behaviour near the bifurcation point (see, for instance, [1, 10], and the references therein). In what follows, we carry out these ideas through the explicit computational procedure found in [14].

To simplify the subsequent computations, we first translate the equilibrium to the origin and normalize the time delay to one. That is, we let $u_1(t) = x(\tau t) - x_*$, $u_2(t) = y(\tau t) - y_*$, and $u_3(t) = z(\tau t) - z_*$. Next, we let $\tau = \tau^* + \nu$, which means that Hopf bifurcation occurs when $\nu = 0$. These transform the system (1) into the following system

$$\begin{cases} \dot{u}_1(t) &=& (\tau^*+\nu)\left[s_1u_1(t)+s_2u_2(t)+s_3u_3(t)\right] \\ && \quad +(\tau^*+\nu)\left[-a_1u_1^2(t)-a_2u_1(t)u_2(t)-a_3u_1(t)u_3(t)\right], \\ \dot{u}_2(t) &=& (\tau^*+\nu)\left[s_4u_2(t)+s_5u_3(t)+r_1u_1(t-1)+r_2u_2(t-1)\right] \\ && \quad +(\tau^*+\nu)\left[b_1e^{-\mu(\tau^*+\nu)}u_1(t-1)u_2(t-1)-b_3u_2(t)u_3(t)\right], \\ \dot{u}_3(t) &=& (\tau^*+\nu)\left[s_6u_1(t)+s_7u_2(t)\right] \\ && \quad +(\tau^*+\nu)\left[c_1u_1(t)u_3(t)+c_2u_2(t)u_3(t)\right], \end{cases} \tag{11}$$

where

$$r_1 = b_1e^{-\mu(\tau^*+\nu)}y_*, \tag{12}$$

$$r_2 = b_1e^{-\mu(\tau^*+\nu)}x_*, \tag{13}$$

and s_i $(i = 1, 2, \dots, 7)$ are as previously defined in equations (4)–(10). The terms in the system (11) were arranged so that it is easier to recognize the linear and nonlinear parts once we rewrite this system as a functional differential equation in $\mathscr{C} = C\left([-1, 0], \mathbb{R}^3\right)$, which is the space of continuous functions mapping $[-1, 0]$ to $\mathbb{R}^3$.

2.1 Abstract Formulation of the System

The first step in the method of Hassard et al. [14] is to write the system (1) as an operator equation, or as an abstract ODE on the phase space $\mathscr{C}$ as most papers like to use. This step makes the linear and nonlinear parts explicit. Let $u(t) = \big(u_1(t), u_2(t), u_3(t)\big)^\top \in \mathbb{R}^3$, and use the notation

$$u_t(\theta) = u(t+\theta) \qquad \text{with} \qquad \theta \in [-1, 0]. \tag{14}$$

Then, the system (11) can be written in the form

$$\dot{u}(t) = L_\nu(u_t) + f(\nu, u_t) \tag{15}$$

where the one-parameter family of continuous linear operator $L_\nu : \mathscr{C} \to \mathbb{R}^3$ is given by

$$L_\nu(\phi) = (\tau^* + \nu) \begin{pmatrix} s_1 & s_2 & s_3 \\ 0 & s_4 & s_5 \\ s_6 & s_7 & 0 \end{pmatrix} \begin{pmatrix} \phi_1(0) \\ \phi_2(0) \\ \phi_3(0) \end{pmatrix} + (\tau^* + \nu) \begin{pmatrix} 0 & 0 & 0 \\ r_1 & r_2 & 0 \\ 0 & 0 & 0 \end{pmatrix} \begin{pmatrix} \phi_1(-1) \\ \phi_2(-1) \\ \phi_3(-1) \end{pmatrix}, \tag{16}$$

while the nonlinear terms beginning with at least the quadratic terms are contained in the function $f : \mathbb{R} \times \mathscr{C} \to \mathbb{R}^3$

$$f(\nu, \phi) = (\tau^* + \nu) \begin{pmatrix} -a_1\phi_1^2(0) - a_2\phi_1(0)\phi_2(0) - a_3\phi_1(0)\phi_3(0) \\ b_1 e^{-\mu(\tau^*+\nu)}\phi_1(-1)\phi_2(-1) - b_3\phi_2(0)\phi_3(0) \\ c_1\phi_1(0)\phi_3(0) + c_2\phi_2(0)\phi_3(0) \end{pmatrix}. \tag{17}$$

By the Riesz Representation Theorem, there exists a 3×3 matrix-valued function $\eta(\theta, \nu)$ of bounded variation for $\theta \in [-1, 0]$ such that

$$L_\nu(\phi) = \int_{-1}^{0} d\eta(\theta, \nu)\phi(\theta) \tag{18}$$

for $\phi \in \mathscr{C}$. In particular, we choose

$$\eta(\theta, \nu) = (\tau^* + \nu) \begin{pmatrix} s_1 & s_2 & s_3 \\ 0 & s_4 & s_5 \\ s_6 & s_7 & 0 \end{pmatrix} \delta(\theta) + (\tau^* + \nu) \begin{pmatrix} 0 & 0 & 0 \\ r_1 & r_2 & 0 \\ 0 & 0 & 0 \end{pmatrix} \delta(\theta + 1), \tag{19}$$

where $\delta(\theta)$ is the Dirac-delta function. Denote by $C^1([-1, 0], \mathbb{R}^3)$ the space of 3-dimensional real vector-valued functions on $[-1, 0]$ all of whose components have continuous first derivatives, and for $\phi \in C^1([-1, 0], \mathbb{R}^3)$, define the operators

$$A(\nu)\phi(\theta) = \begin{cases} \dfrac{d\phi(\theta)}{d\theta} & \text{if} \quad \theta \in [-1, 0), \\ \displaystyle\int_{-1}^{0} d\eta(s, \nu)\phi(s) & \text{if} \quad \theta = 0, \end{cases} \tag{20}$$

and

$$R(\nu)\phi(\theta) = \begin{cases} 0 & \text{if} \quad \theta \in [-1, 0), \\ f(\nu, \phi) & \text{if} \quad \theta = 0. \end{cases} \tag{21}$$

Using equations (20) and (21), and since $\frac{d}{dt}u_t = \frac{d}{d\theta}u_t$ from equation (14), the system (15) is then equivalent to the following operator equation

$$\dot{u}_t = A(\nu)u_t + R(\nu)u_t. \tag{22}$$

For the remainder of this section, we only consider the case when $\nu = 0$, that is, when the system (1) undergoes a Hopf bifurcation around the coexistence equilibrium E_*. Notice that since $\pm i\omega$ are the eigenvalues of the original system (1) at E_*, then $\pm i\omega\tau^*$ are the eigenvalues of $A(0)$.

2.2 Centre Manifold Reduction

The second step in the method of Hassard et al. [14] is to project the system, which so far we have written as an abstract ODE given in equation (22), into the two-dimensional centre manifold C_0. Recall that at the critical value $\nu = 0$, the operator $A(0)$ has a simple pair of purely imaginary eigenvalues $\pm i\omega\tau^*$, while all remaining eigenvalues lie in the open left-half plane. Hence, the local dynamics near the Hopf bifurcation point are determined by the flow on a two-dimensional centre manifold tangent to the eigenspace associated with these critical eigenvalues. The purpose of this step is to introduce coordinates on that centre manifold and derive the corresponding reduced equation. Key to this process is the bilinear form, due to Hale [13], which allows us to obtain local coordinates in C_0 and eventually write the reduced equations in C_0. Denote by $\mathbb{R}^{3*}$ the real 3-dimensional space of row vectors, and for $\psi \in C^1([0, 1], \mathbb{R}^{3*})$, define A^* as follows

$$A^*\psi(s) = \begin{cases} -\dfrac{d\psi(s)}{ds} & \text{if} \quad s \in (0, 1], \\ \displaystyle\int_{-1}^{0} d\eta^\top(t, 0)\psi(-t) & \text{if} \quad s = 0. \end{cases} \tag{23}$$

For $\phi \in \mathscr{C}$ and $\psi \in \mathscr{C}^* = C([0, 1], \mathbb{R}^{3*})$, we also define the following bilinear form

$$\langle \psi(s), \phi(\theta) \rangle = \overline{\psi}(0)\phi(0) - \int_{\theta=-1}^{0} \int_{\xi=0}^{\theta} \overline{\psi}(\xi - \theta) d\eta(\theta)\phi(\xi)d\xi \tag{24}$$

where $\eta(\theta) = \eta(\theta, 0)$. The operator A^*, given in the equation (23), is referred to in the literature as the formal adjoint of $A(0)$ relative to the bilinear form (24), see, e.g. [12, pp.50] and [13, pp.173]. It can be shown that the bilinear form given in equation (24) satisfies the following properties

$$\langle \psi, \lambda\phi \rangle = \lambda\langle \psi, \phi \rangle, \qquad \langle \lambda\psi, \phi \rangle = \overline{\lambda}\langle \psi, \phi \rangle \qquad \text{and} \qquad \langle \psi, A\phi \rangle = \langle A^*\psi, \phi \rangle. \tag{25}$$

Since $\pm i\omega\tau^*$ are eigenvalues of $A(0)$, and $A(0)$ and A^* are adjoint operators, then $\pm i\omega\tau^*$ are also eigenvalues of A^*. We now compute the eigenvector $q(\theta)$ corresponding to the eigenvalue $i\omega\tau^*$ of $A(0)$, as well as the eigenvector $q^*(s)$ corresponding to the eigenvalue $-i\omega\tau^*$ of A^*. Note that for $\theta \in [-1, 0)$, we get $A(0)q(\theta) = \frac{d}{d\theta}q(\theta)$ using the equation (20) with $\nu = 0$. So, the eigenvalue equation

$$A(0)q(\theta) = i\omega\tau^* q(\theta) \tag{26}$$

yields $\frac{d}{d\theta}q(\theta) = i\omega\tau^* q(\theta)$, that is, $q(\theta) = q(0)e^{i\omega\tau^*\theta}$. To simplify the computations, we let $q(0) = (1, \alpha, \beta)^\top$, so that the eigenvector $q(\theta)$ of $A(0)$ corresponding to the eigenvalue $i\omega\tau^*$ takes the following form

$$q(\theta) = (1, \alpha, \beta)^\top e^{i\omega\tau^*\theta}. \tag{27}$$

Using the expression for $A(0)$ with $\theta = 0$ from equations (20), (18) and (16), together with the fact that $q(-1) = q(0)e^{-i\omega\tau^*}$, the eigenvalue equation (26) gives

$$\tau^* \begin{pmatrix} s_1 - i\omega & s_2 & s_3 \\ r_1 e^{-i\omega\tau^*} & s_4 - i\omega + r_2 e^{-i\omega\tau^*} & s_5 \\ s_6 & s_7 & -i\omega \end{pmatrix} q(0) = \begin{pmatrix} 0 \\ 0 \\ 0 \end{pmatrix}.$$

Consequently, we have

$$q(0) = (1, \alpha, \beta)^\top = \left(1, \frac{s_3 r_1 e^{-i\omega\tau^*} - s_5(s_1 - i\omega)}{s_2 s_5 - s_3(s_4 - i\omega + r_2 e^{-i\omega\tau^*})}, \frac{s_6 + \alpha s_7}{i\omega}\right)^\top, \tag{28}$$

and the eigenvector $q(\theta)$ given in the equation (27) is now obtained. Similarly, one can show, using the equation (23) for $s \in (0, 1]$, that the eigenvector $q^*(s)$ corresponding to the eigenvalue $-i\omega\tau^*$ of A^* takes the form

$$q^*(s) = D(1, \alpha^*, \beta^*)e^{i\omega\tau^* s}, \tag{29}$$

and the corresponding eigenvalue equation gives

$$q^*(0) = D(1, \alpha^*, \beta^*) = D\left(1, \frac{s_2 s_6 - s_7(s_1 + i\omega)}{s_7 r_1 e^{i\omega\tau^*} - s_6(s_4 + i\omega + r_2 e^{i\omega\tau^*})}, \frac{s_3 + \alpha^* s_5}{-i\omega}\right). \tag{30}$$

In view of the normalization of $q^*(s)$ and $q(\theta)$, we must choose D such that $\langle q^*(s), q(\theta)\rangle = 1$. Using the bilinear form in equation (24), we have

$$
\begin{aligned}
\langle q^*(s), q(\theta)\rangle &= \overline{D}(1, \overline{\alpha^*}, \overline{\beta^*})\ (1, \alpha, \beta)^\top \\
&\quad - \int_{\theta=-1}^{0} \int_{\xi=0}^{\theta} \overline{D}(1, \overline{\alpha^*}, \overline{\beta^*})\ e^{-i\omega\tau^*(\xi-\theta)}\ d\eta(\theta)\ (1, \alpha, \beta)^\top\ e^{i\omega\tau^*\xi}\ d\xi \\
&= \overline{D}\left\{1 + \overline{\alpha^*}\alpha + \overline{\beta^*}\beta - \int_{-1}^{0} (1, \overline{\alpha^*}, \overline{\beta^*})\ d\eta(\theta)\ \theta e^{i\omega\tau^*\theta}\ (1, \alpha, \beta)^\top\right\} \\
&= \overline{D}\left\{1 + \alpha\overline{\alpha^*} + \beta\overline{\beta^*} + \overline{\alpha^*}\,(r_1 + \alpha r_2)\,\tau^* e^{-i\omega\tau^*}\right\}.
\end{aligned}
$$

Thus, when

$$
D = \frac{1}{1 + \overline{\alpha}\alpha^* + \overline{\beta}\beta^* + \alpha^*(r_1 + \overline{\alpha}r_2)\tau^* e^{i\omega\tau^*}}, \tag{31}
$$

we get $\langle q^*(s), q(\theta)\rangle = 1$. Moreover, using the properties of the bilinear form enumerated in equation (25), one can show by direct computation that $\langle q^*(s), \overline{q}(\theta)\rangle = 0$.

Delay differential equations, like the system (1), are infinite-dimensional problems. However, at the bifurcation point where $\nu = 0$, all eigenvalues of $A(0)$ have a negative real part, except for the simple pair that are on the imaginary axis. This allows us to project the infinite-dimensional problem to the centre manifold C_0, which is a two-dimensional invariant manifold tangent at the origin to the centre subspace spanned by the eigenvectors corresponding to the purely imaginary eigenvalues of $A(0)$. Therefore, the local dynamics of the system near the Hopf bifurcation point are determined by the flow restricted to C_0.

We now derive the reduced equations on the centre manifold C_0. Let u_t be a solution of the operator equation (22) when $\nu = 0$, and define the following

$$
z(t) = \langle q^*, u_t\rangle \tag{32}
$$

and

$$
W(t, \theta) = u_t(\theta) - z(t)q(\theta) - \overline{z}(t)\overline{q}(\theta) = u_t(\theta) - 2\mathrm{Re}\left\{z(t)q(\theta)\right\}. \tag{33}
$$

In the centre manifold C_0, we have

$$
W(t, \theta) = W\left(z(t), \overline{z}(t), \theta\right) = W_{20}(\theta)\frac{z^2}{2} + W_{11}(\theta)z\overline{z} + W_{02}(\theta)\frac{\overline{z}^2}{2} + \cdots, \tag{34}
$$

where z and $\overline{z}$ are local coordinates on the centre manifold C_0 in the direction of q^* and $\overline{q^*}$. The quantity $z(t)$ measures the component of the state u_t along the critical eigendirection, while $W(t, \theta)$ represents the remaining component transverse to the centre subspace. Thus, equation (32) introduces a local coordinate on the centre manifold, and equation (33) decomposes the state into its centre part and its transverse part. On the centre manifold, the transverse component depends smoothly on the centre variables $(z, \overline{z})$. Hence, the expansion in equation (34) gives a local parametrization of the centre manifold near the origin, reducing the original infinite-dimensional system to a finite-dimensional one in the variables z and $\overline{z}$. Differentiating $z(t)$ from the equation (32) and then using the form for $\dot{u}_t$ from the equation (22) with $\nu = 0$, we get

$$\dot{z}(t) = \langle q^*, A(0)u_t \rangle + \langle q^*, R(0)u_t \rangle. \tag{35}$$

It can be shown that

$$\langle q^*, A(0)u_t \rangle = i\omega\tau^* z \tag{36}$$

using the properties of the bilinear form given in the equation (25). Meanwhile,

$$\langle q^*, R(0)u_t \rangle = \overline{q^*}(0) f(0, u_t(0))$$

using the bilinear form in equation (24) and observing that the term with integrals vanishes by using the properties of $R(\nu)$ with $\nu = 0$ in equation (21). From equation (33) with $\theta = 0$, we get $u_t(0) = W(t,0) + 2\mathrm{Re}\,\{z(t)q(0)\}$, and consequently

$$\langle q^*, R(0)u_t \rangle = \overline{q^*}(0) f\big(0, W(z(t), \overline{z}(t), 0) + 2\mathrm{Re}\,\{z(t)q(0)\}\,\big). \tag{37}$$

Substituting the quantities from equations (36) and (37) to equation (35), we obtain the following reduced equation in the centre manifold C_0

$$\dot{z}(t) = \; i\omega\tau^* z \; + \; g(z, \overline{z}) \tag{38}$$

with

$$g(z, \overline{z}) = \overline{q^*}(0) f_0(z, \overline{z}), \tag{39}$$

and where $f_0(z, \overline{z}) = f\left(0, W(z(t), \overline{z}(t), 0) + 2\mathrm{Re}\,\{z(t)q(0)\}\right)$. The function g in the reduced equation (38) contains the nonlinear terms and thus can be written as

$$g(z, \overline{z}) = \tfrac{1}{2} g_{20} z^2 + g_{11} z\overline{z} + \tfrac{1}{2} g_{02} \overline{z}^2 + \tfrac{1}{2} g_{21} z^2 \overline{z} + \cdots . \tag{40}$$

2.3 Normal Form Calculation on the Centre Manifold

The third and last step in the method of Hassard et al. [14] is using the normal form theory to the reduced equation in the centre manifold given in equation (38). The role of the normal form calculation is to simplify the reduced system and isolate the coefficients that determine the local behaviour of the Hopf bifurcation. In the following, we compute for the coefficients g_{20}, g_{11}, g_{02} and g_{21} given in equation (40). Using equations (33) and (34), we have

$$u_t(\theta) = W(z(t), \overline{z}(t), \theta) + z(t)q(\theta) + \overline{z}(t)\overline{q}(\theta). \tag{41}$$

Note that the left-hand side of the equation (41) is $u_t(\theta) = (\phi_1(\theta), \phi_2(\theta), \phi_3(\theta))^\top$, while the right-hand side of the equation (41) can be computed using $W(z(t), \overline{z}(t), \theta)$ from equation (34) and $q(\theta)$ from equation (27). The following expressions were obtained from equation

(41), considering the cases where $\theta = 0$ and where $\theta = -1$:

$$\begin{aligned}
\phi_1(0) &= z + \overline{z} + W_{20}^{(1)}(0)\frac{z^2}{2} + W_{11}^{(1)}(0)z\overline{z} + W_{02}^{(1)}(0)\frac{\overline{z}^2}{2} + \cdots\,,\\
\phi_2(0) &= z\alpha + \overline{z\alpha} + W_{20}^{(2)}(0)\frac{z^2}{2} + W_{11}^{(2)}(0)z\overline{z} + W_{02}^{(2)}(0)\frac{\overline{z}^2}{2} + \cdots\,,\\
\phi_3(0) &= z\beta + \overline{z\beta} + W_{20}^{(3)}(0)\frac{z^2}{2} + W_{11}^{(3)}(0)z\overline{z} + W_{02}^{(3)}(0)\frac{\overline{z}^2}{2} + \cdots\,,\\
\phi_1(-1) &= ze^{-i\omega\tau^*} + \overline{z}e^{i\omega\tau^*} + W_{20}^{(1)}(-1)\frac{z^2}{2} + W_{11}^{(1)}(-1)z\overline{z} + W_{02}^{(1)}(-1)\frac{\overline{z}^2}{2} + \cdots\,,\\
\phi_2(-1) &= z\alpha e^{-i\omega\tau^*} + \overline{z\alpha}e^{i\omega\tau^*} + W_{20}^{(2)}(-1)\frac{z^2}{2} + W_{11}^{(2)}(-1)z\overline{z} + W_{02}^{(2)}(-1)\frac{\overline{z}^2}{2} + \cdots\,.
\end{aligned}$$

Consequently, we obtain the following quantities

$$\begin{aligned}
{\phi_1}^2(0) &= z^2 + \overline{z}^2 + 2z\overline{z} + \big(W_{20}^{(1)}(0) + 2W_{11}^{(1)}(0)\big)z^2\overline{z} + \cdots\,,\\
\phi_1(0)\phi_2(0) &= \alpha z^2 + \overline{\alpha z}^2 + (\alpha + \overline{\alpha})z\overline{z}\\
&\quad + \big(\tfrac{1}{2}W_{20}^{(2)}(0) + W_{11}^{(2)}(0) + \tfrac{1}{2}\overline{\alpha}W_{20}^{(1)}(0) + \alpha W_{11}^{(1)}(0)\big)z^2\overline{z} + \cdots\,,\\
\phi_1(0)\phi_3(0) &= \beta z^2 + \overline{\beta}\overline{z}^2 + (\beta + \overline{\beta})z\overline{z}\\
&\quad + \big(\tfrac{1}{2}W_{20}^{(3)}(0) + W_{11}^{(3)}(0) + \tfrac{1}{2}\overline{\beta}W_{20}^{(1)}(0) + \beta W_{11}^{(1)}(0)\big)z^2\overline{z} + \cdots\,,\\
\phi_2(0)\phi_3(0) &= \alpha\beta z^2 + \overline{\alpha\beta}\overline{z}^2 + (\overline{\alpha}\beta + \alpha\overline{\beta})z\overline{z}\\
&\quad + \big(\tfrac{1}{2}\overline{\alpha}W_{20}^{(3)}(0) + \alpha W_{11}^{(3)}(0) + \tfrac{1}{2}\overline{\beta}W_{20}^{(2)}(0) + \beta W_{11}^{(2)}(0)\big)z^2\overline{z} + \cdots\,,\\
\phi_1(-1)\phi_2(-1) &= \alpha e^{-2i\omega\tau^*}z^2 + \overline{\alpha}e^{2i\omega\tau^*}\overline{z}^2 + (\alpha + \overline{\alpha})z\overline{z}\\
&\quad + \big(\tfrac{1}{2}e^{i\omega\tau^*}W_{20}^{(2)}(-1) + e^{-i\omega\tau^*}W_{11}^{(2)}(-1) + \tfrac{1}{2}\overline{\alpha}e^{i\omega\tau^*}W_{20}^{(1)}(-1)\\
&\quad + \alpha e^{-i\omega\tau^*}W_{11}^{(1)}(-1)\big)z^2\overline{z} + \cdots\,.
\end{aligned}$$

To obtain an expression for $g(z,\overline{z})$ from equation (39), we can use equations (29) and (17) to get the respective expressions for $\overline{q^*}(0)$ and $f_0(z,\overline{z})$. This yields

$$\begin{aligned}
g(z,\overline{z}) = \tau^*\overline{D}\big[&-a_1\phi_1^2(0) - a_2\phi_1(0)\phi_2(0) + (\overline{\beta^*}c_1 - a_3)\phi_1(0)\phi_3(0)\\
&+ (\overline{\beta^*}c_2 - \overline{\alpha^*}b_3)\phi_2(0)\phi_3(0) + \overline{\alpha^*}b_1e^{-\mu\tau^*}\phi_1(-1)\phi_2(-1)\big].
\end{aligned} \tag{42}$$

As previously computed, the expressions for $\phi_1^2(0)$, $\phi_1(0)\phi_2(0)$, $\phi_1(0)\phi_3(0)$, $\phi_2(0)\phi_3(0)$ and $\phi_1(-1)\phi_2(-1)$ are all in terms z and $\overline{z}$. So the right-hand side of the equation (42) is in terms of z and $\overline{z}$ as well. Now, comparing coefficients between the equations (40) and (42), we obtain

$$
\begin{aligned}
g_{20} &= 2\tau^*\overline{D}\big\{-a_1-\alpha a_2+\beta(\overline{\beta^*}c_1-a_3)+\alpha\beta(\overline{\beta^*}c_2-\overline{\alpha^*}b_3)+(\alpha e^{-2i\omega\tau^*})(\overline{\alpha^*}b_1e^{-\mu\tau^*})\big\},\\
g_{11} &= \tau^*\overline{D}\big\{-2a_1-(\alpha+\overline{\alpha})a_2+(\beta+\overline{\beta})(\overline{\beta^*}c_1-a_3)+(\overline{\alpha}\beta+\alpha\overline{\beta})(\overline{\beta^*}c_2-\overline{\alpha^*}b_3)\\
&\qquad\quad+(\alpha+\overline{\alpha})(\overline{\alpha^*}b_1e^{-\mu\tau^*})\big\},\\
g_{02} &= 2\tau^*\overline{D}\big\{-a_1-\overline{\alpha}a_2+\overline{\beta}(\overline{\beta^*}c_1-a_3)+\overline{\alpha\beta}(\overline{\beta^*}c_2-\overline{\alpha^*}b_3)+(\overline{\alpha}e^{2i\omega\tau^*})(\overline{\alpha^*}b_1e^{-\mu\tau^*})\big\},\\
g_{21} &= 2\tau^*\overline{D}\big\{-\big(W_{20}^{(1)}(0)+2W_{11}^{(1)}(0)\big)a_1-\big(\tfrac{1}{2}W_{20}^{(2)}(0)+W_{11}^{(2)}(0)+\tfrac{1}{2}\overline{\alpha}W_{20}^{(1)}(0)\\
&\quad+\alpha W_{11}^{(1)}(0)\big)a_2+\big(\tfrac{1}{2}W_{20}^{(3)}(0)+W_{11}^{(3)}(0)+\tfrac{1}{2}\overline{\beta}W_{20}^{(1)}(0)+\beta W_{11}^{(1)}(0)\big)(\overline{\beta^*}c_1-a_3)\\
&\quad+\big(\tfrac{1}{2}\overline{\alpha}W_{20}^{(3)}(0)+\alpha W_{11}^{(3)}(0)+\tfrac{1}{2}\overline{\beta}W_{20}^{(2)}(0)+\beta W_{11}^{(2)}(0)\big)(\overline{\beta^*}c_2-\overline{\alpha^*}b_3)\\
&\quad+\big(\tfrac{1}{2}e^{i\omega\tau^*}W_{20}^{(2)}(-1)+e^{-i\omega\tau^*}W_{11}^{(2)}(-1)+\tfrac{1}{2}\overline{\alpha}e^{i\omega\tau^*}W_{20}^{(1)}(-1)\\
&\quad\;+\alpha e^{-i\omega\tau^*}W_{11}^{(1)}(-1)\big)(\overline{\alpha^*}b_1e^{-\mu\tau^*})\big\}.
\end{aligned}
$$

We still need to compute for $W_{20}(\theta)$ and $W_{11}(\theta)$ because they appear in the coefficient g_{21}. From equation (33), we have $u_t(\theta)=W(t,\theta)+z(t)q(\theta)+\overline{z}(t)\overline{q}(\theta)$, and thus

$$\dot{u}_t(\theta)=\dot{W}(t,\theta)+\dot{z}(t)q(\theta)+\dot{\overline{z}}(t)\overline{q}(\theta). \tag{43}$$

If $\theta\in[-1,0)$, then from equation (22) with $\nu=0$, we get $\dot{u}_t(\theta)=A(0)u_t(\theta)$. Meanwhile, using equations (33) and (26), we get

$$\dot{u}_t(\theta)=A(0)W(t,\theta)+z(t)\left(i\omega\tau^*q(\theta)\right)+\overline{z}(t)\left(-i\omega\tau^*\overline{q}(\theta)\right). \tag{44}$$

Equations (43) and (44) give an expression for $\dot{W}(t,\theta)$, which after using equations (38) and (39) becomes $\dot{W}(t,\theta)=A(0)W(t,\theta)-2\mathrm{Re}\left\{\overline{q^*}(0)f_0(z,\overline{z})q(\theta)\right\}$. Following a similar process for the case where $\theta=0$, we get $\dot{W}(t,\theta)=A(0)W(t,\theta)-2\mathrm{Re}\left\{\overline{q^*}(0)f_0(z,\overline{z})q(\theta)\right\}+f(0,u_t(\theta))$. Therefore,

$$\dot{W}(z,\overline{z},\theta)=\begin{cases}A(0)W(z,\overline{z},\theta)-2\mathrm{Re}\{\overline{q^*}(0)f_0(z,\overline{z})q(\theta)\}, & \text{if}\quad \theta\in[-1,0),\\ A(0)W(z,\overline{z},\theta)-2\mathrm{Re}\{\overline{q^*}(0)f_0(z,\overline{z})q(\theta)\}+f_0(z,\overline{z}), & \text{if}\quad \theta=0.\end{cases} \tag{45}$$

We rewrite equation (45) as follows

$$\dot{W}(z,\overline{z},\theta)=A(0)W(z,\overline{z},\theta)+H(z,\overline{z},\theta) \tag{46}$$

where the higher-order terms are

$$H(z,\overline{z},\theta)=H_{20}(\theta)\frac{z^2}{2}+H_{11}(\theta)z\overline{z}+H_{02}(\theta)\frac{\overline{z}^2}{2}+\cdots. \tag{47}$$

Using the expressions for $W(z,\overline{z},\theta)$ and $H(z,\overline{z},\theta)$ from the equations (34) and (47), respectively, the right-hand side of equation (46) then becomes

$$A(0)W(z,\overline{z},\theta)+H(z,\overline{z},\theta)=\left[A(0)W_{20}(\theta)+H_{20}(\theta)\right]\frac{z^2}{2}+\left[A(0)W_{11}(\theta)+H_{11}(\theta)\right]z\overline{z}+\cdots. \tag{48}$$

Meanwhile, in the centre manifold C_0 near the origin, we have $\dot{W}=W_z\dot{z}+W_{\overline{z}}\dot{\overline{z}}$. Hence, the left-hand side of the equation (46) is

$$\dot{W}(z,\overline{z},\theta)=\left[i\omega\tau^* zW_{20}(\theta)\right]z^2+[0]\,z\overline{z}+\cdots. \tag{49}$$

Matching the corresponding coefficients in equations (48) and (49), specifically those terms with z^2 and those with $z\overline{z}$, we get

$$A(0)W_{20}(\theta)=2i\omega\tau^* W_{20}(\theta)-H_{20}(\theta), \tag{50}$$

$$A(0)W_{11}(\theta)=-H_{11}(\theta). \tag{51}$$

For the case where $\theta\in[-1,0)$ in the equation (45), together with the equation (39), we obtain $H(z,\overline{z},\theta)=-g(z,\overline{z})q(\theta)-\overline{g}(z,\overline{z})\overline{q}(\theta)$. That is,

$$H(z,\overline{z},\theta)=-\tfrac{1}{2}\left[g_{20}q(\theta)+\overline{g}_{02}\overline{q}(\theta)\right]z^2-\left[g_{11}q(\theta)+\overline{g}_{11}\overline{q}(\theta)\right]z\overline{z}+\cdots. \tag{52}$$

By comparing the coefficients in equation (52) with the coefficients in equation (47), we get

$$-H_{20}(\theta)=g_{20}q(\theta)+\overline{g}_{02}\overline{q}(\theta), \tag{53}$$

$$-H_{11}(\theta)=g_{11}q(\theta)+\overline{g}_{11}\overline{q}(\theta). \tag{54}$$

Now, using the definition of $A(0)$ for $\theta\in[-1,0)$ from the equation (20) and the expressions for $H_{20}(\theta)$ and $H_{11}(\theta)$ from the equations (53) and (54), we obtain from the equations (50) and (51) the following differential equations

$$\dot{W}_{20}(\theta)=2i\omega\tau^* W_{20}(\theta)+g_{20}q(\theta)+\overline{g}_{02}\overline{q}(\theta), \tag{55}$$

$$\dot{W}_{11}(\theta)=g_{11}q(\theta)+\overline{g}_{11}\overline{q}(\theta). \tag{56}$$

Note that $q(\theta)=q(0)e^{i\omega\tau^*\theta}$. Thus, we can solve the differential equations (55) and (56) and obtain

$$W_{20}(\theta)=\frac{g_{20}}{-i\omega\tau^*}q(0)e^{i\omega\tau^*\theta}+\frac{\overline{g}_{02}}{-3i\omega\tau^*}\overline{q}(0)e^{-i\omega\tau^*\theta}+M_1e^{2i\omega\tau^*\theta}, \tag{57}$$

$$W_{11}(\theta)=\frac{g_{11}}{i\omega\tau^*}q(0)e^{i\omega\tau^*\theta}+\frac{\overline{g}_{11}}{-i\omega\tau^*}\overline{q}(0)e^{-i\omega\tau^*\theta}+M_2, \tag{58}$$

where M_1 and M_2 are constant vectors that need to be computed. Using the definition of

$A(0)$ for $\theta = 0$ from equation (20) in equations (50) and (51), we get

$$\int_{-1}^{0} d\eta(\theta)W_{20}(\theta) = 2i\omega\tau^* W_{20}(0) - H_{20}(0), \tag{59}$$

$$\int_{-1}^{0} d\eta(\theta)W_{11}(\theta) = -H_{11}(0), \tag{60}$$

where $\eta(\theta) = \eta(\theta, 0)$. We claim that M_1 can be obtained by expanding the left-hand side and the right-hand side of the equation (59), and the same goes for computing M_2 from the equation (60). For the case where $\theta = 0$ in the equation (45), together with the equation (39), we get $H(z, \overline{z}, 0) = -g(z, \overline{z})q(0) - \overline{g}(z, \overline{z})\overline{q}(0) + f_0(z, \overline{z})$. That is,

$$\begin{aligned} H(z, \overline{z}, 0) = &- \left[g_{20}q(0) + \overline{g}_{02}\overline{q}(0)\right] \frac{z^2}{2} - \left[g_{11}q(0) + \overline{g}_{11}\overline{q}(0)\right] z\overline{z} + \cdots \\ &+ \tau^* \begin{bmatrix} (-a_1 - a_2\alpha - a_3\beta)\, z^2 + \left(-2a_1 - a_2(\alpha + \overline{\alpha}) - a_3(\beta + \overline{\beta})\right) z\overline{z} + \cdots \\ \left(b_1 e^{-\mu\tau^*} \alpha e^{-2i\omega\tau^*} - b_3\alpha\beta\right) z^2 + \left(b_1 e^{-\mu\tau^*}(\alpha + \overline{\alpha}) - b_3(\overline{\alpha}\beta + \alpha\overline{\beta})\right) z\overline{z} + \cdots \\ (c_1\beta + c_2\alpha\beta)\, z^2 + \left(c_1(\beta + \overline{\beta}) + c_2(\overline{\alpha}\beta + \alpha\overline{\beta})\right) z\overline{z} + \cdots \end{bmatrix}. \end{aligned}$$

By comparing coefficients with the equation (47), i.e. the case with $\theta = 0$, we have

$$H_{20}(0) = -g_{20}q(0) - \overline{g}_{02}\overline{q}(0) + 2\tau^* \begin{bmatrix} -a_1 - \alpha a_2 - \beta a_3 \\ \left(\alpha e^{-2i\omega\tau^*}\right) b_1 e^{-\mu\tau^*} - \alpha\beta b_3 \\ \beta c_1 + \alpha\beta c_2 \end{bmatrix}, \tag{61}$$

$$H_{11}(0) = -g_{11}q(0) - \overline{g}_{11}\overline{q}(0) + \tau^* \begin{bmatrix} -2a_1 - (\alpha + \overline{\alpha})\, a_2 - \left(\beta + \overline{\beta}\right) a_3 \\ (\alpha + \overline{\alpha})\, b_1 e^{-\mu\tau^*} - \left(\overline{\alpha}\beta + \alpha\overline{\beta}\right) b_3 \\ \left(\beta + \overline{\beta}\right) c_1 + \left(\overline{\alpha}\beta + \alpha\overline{\beta}\right) c_2 \end{bmatrix}. \tag{62}$$

Using the expressions for $W_{20}(0)$ and $H_{20}(0)$ from the equations (57) and (61), respectively, the right-hand side of equation (59) becomes

$$\begin{aligned} 2i\omega\tau^* W_{20}(0) - H_{20}(0) = &-g_{20}q(0) + \tfrac{1}{3}\overline{g}_{02}\overline{q}(0) + 2i\omega\tau^* M_1 \\ &- 2\tau^* \begin{bmatrix} -a_1 - \alpha a_2 - \beta a_3 \\ \left(\alpha e^{-2i\omega\tau^*}\right) b_1 e^{-\mu\tau^*} - \alpha\beta b_3 \\ \beta c_1 + \alpha\beta c_2 \end{bmatrix}. \end{aligned} \tag{63}$$

As for the left-hand side, first note that

$$\int_{-1}^{0} d\eta(\theta)q(0)e^{i\omega\tau^*\theta} = i\omega\tau^* q(0) \qquad \text{and} \qquad \int_{-1}^{0} d\eta(\theta)\overline{q}(0)e^{-i\omega\tau^*\theta} = -i\omega\tau^*\overline{q}(0) \tag{64}$$

which are derived from the eigenvalue equation (26) with $\theta = 0$. Now, using equation (57) to the left-hand side of equation (59), together with the relations in equation (64), as well as the expression for L_0 in equations (18) and (16), we get

$$\int_{-1}^{0} d\eta(\theta)W_{20}(\theta) = -g_{20}q(0) + \tfrac{1}{3}\overline{g}_{02}\overline{q}(0) + \tau^* \begin{bmatrix} s_1 & s_2 & s_3 \\ 0 & s_4 & s_5 \\ s_6 & s_7 & 0 \end{bmatrix} M_1 + \tau^* \begin{bmatrix} 0 & 0 & 0 \\ r_1 & r_2 & 0 \\ 0 & 0 & 0 \end{bmatrix} M_1 e^{-2i\omega\tau^*}. \tag{65}$$

Therefore, matching the right-hand side given in equation (63) and the left-hand side given in equation (65), we obtain

$$\begin{bmatrix} 2i\omega - s_1 & -s_2 & -s_3 \\ -r_1 e^{-2i\omega\tau^*} & 2i\omega - s_4 - r_2 e^{-2i\omega\tau^*} & -s_5 \\ -s_6 & -s_7 & 2i\omega \end{bmatrix} M_1 = 2 \begin{bmatrix} -a_1 - \alpha a_2 - \beta a_3 \\ \alpha b_1 e^{-2i\omega\tau^*} e^{-\mu\tau^*} - \alpha\beta b_3 \\ \beta c_1 + \alpha\beta c_2 \end{bmatrix}. \tag{66}$$

By a similar process, i.e., expanding both sides of the equation (60) and utilizing equations (58) and (62), we also obtain

$$\begin{bmatrix} s_1 & s_2 & s_3 \\ r_1 & s_4 + r_2 & s_5 \\ s_6 & s_7 & 0 \end{bmatrix} M_2 = - \begin{bmatrix} -2a_1 - (\alpha + \overline{\alpha})\, a_2 - \left(\beta + \overline{\beta}\right) a_3 \\ (\alpha + \overline{\alpha}) \left(b_1 e^{-\mu\tau^*}\right) - \left(\overline{\alpha}\beta + \alpha\overline{\beta}\right) b_3 \\ \left(\beta + \overline{\beta}\right) c_1 + \left(\overline{\alpha}\beta + \alpha\overline{\beta}\right) c_2 \end{bmatrix}. \tag{67}$$

Solving for M_1 and M_2 from equations (66) and (67) gives the value of the coefficient g_{21}.

2.4 Criticality and Stability of the Hopf Bifurcation

We can now compute the coefficients g_{20}, g_{11}, g_{02} and g_{21}, as well as these quantities [14]:

$$c_1(0) = \frac{i}{2\omega\tau^*}\left(g_{20}g_{11} - 2|g_{11}|^2 - \tfrac{1}{3}|g_{02}|^2\right) + \tfrac{1}{2}g_{21}, \tag{68}$$

$$\mu_2 = -\frac{\mathrm{Re}\{c_1(0)\}}{\mathrm{Re}\{\lambda'(\tau^*)\}}, \tag{69}$$

$$\beta_2 = 2\mathrm{Re}\{c_1(0)\}. \tag{70}$$

We have the following result on the criticality of the Hopf bifurcation around the coexistence equilibrium E_* of the system (1) when $\tau = \tau^*$, as well as on the stability of the periodic solutions born from the Hopf bifurcation.

Theorem 2.1. *Suppose that the system* (1) *undergoes a Hopf bifurcation around the coexistence equilibrium E_* when $\tau = \tau^*$. Then, this Hopf bifurcation has the following qualities:*

A. *The quantity μ_2, given in the equation* (69)*, determines the criticality or the direction of the Hopf bifurcation. If $\mu_2 > 0$ (resp., $\mu_2 < 0$), then the Hopf bifurcation is supercritical (resp., subcritical) and the bifurcating periodic solutions exist for $\tau > \tau^*$ (resp., $\tau < \tau^*$).*

B. *The value of the Floquet exponent β_2, given in the equation* (70)*, determines the stability of the bifurcating periodic solutions. The bifurcating periodic solutions are orbitally asymptotically stable (resp., unstable) if $\beta_2 < 0$ (resp., $\beta_2 > 0$).*

To illustrate Theorem 2.1, we utilize, for the system (1), the same set of parameter values as in [6] where $a_0 = 5.00$, $a_1 = 0.40$, $a_2 = 1.00$, $a_3 = 0.85$, $b_0 = 1.00$, $b_1 = 1.00$, $b_3 = 1.00$, $c_0 = 1.20$, $c_1 = 0.10$, $c_2 = 1.00$, and $\mu = 0.01$. This gives the critical time-delay values

$$\tau_0^- \approx 1.0515 \qquad \text{and} \qquad \tau_1^+ \approx 2.4002$$

where the system (1) undergoes Hopf bifurcations around the coexistence equilibrium E_*. Furthermore, at $\tau = \tau_0^-$, the coexistence equilibrium E_* switched from being unstable to being locally asymptotically stable (LAS), whereas at $\tau = \tau_1^+$, the coexistence equilibrium E_* switched from being LAS to being unstable. In other words, the roots of the characteristic equation (3) that are on the imaginary axis when $\tau = \tau_0^-$ will move towards the open left-half of the complex plane. That is,

$$\mathrm{Re}\{\lambda'(\tau_0^-)\} < 0. \tag{71}$$

Meanwhile, the characteristic roots that are on the imaginary axis when $\tau = \tau_1^+$ will move towards the open right-half of the complex plane, or equivalently,

$$\mathrm{Re}\{\lambda'(\tau_1^+)\} > 0. \tag{72}$$

Example 1. We first determine the qualities of the first Hopf bifurcation, i.e., when $\tau^* = \tau_0^-$. To compute the value of $c_1(0)$, given in the equation (68), we must obtain the values of the following quantities in the following order: $s_i (i = 1, \dots, 7)$ from the equations (4)-(10), and r_1 and r_2 from the equations (12) and (13); the components of eigenvectors $q(0)$ and $q^*(0)$ from the equations (27) and (29); the value of D from the equation (31); the vectors M_1 and M_2 from the equations (66) and (67); $W_{20}(\theta)$ and $W_{11}(\theta)$ from equations (57) and (58) and their evaluation when $\theta = 0$ and when $\theta = -1$. Finally, we can compute the coefficients g_{20}, g_{11}, g_{02}, and g_{21} of the nonlinear part $g(z, \overline{z})$ in the reduced equation in the centre manifold given in equation (38). For the first Hopf bifurcation, that is, when $\tau^* = \tau_0^-$, we obtain

$$c_1(0) \approx -0.0356 - 0.0307i.$$

Consequently, $\mathrm{Re}\{c_1(0)\} < 0$. Since $\mathrm{Re}\{\lambda'(\tau_0^-)\} < 0$ from the equation (71), we see that μ_2 from the equation (69) is negative. Moreover, β_2 given in the equation (70) is negative because $\mathrm{Re}\{c_1(0)\} < 0$. Therefore, since

$$\mu_2 < 0 \qquad \text{and} \qquad \beta_2 < 0,$$

Theorem 2.1 tells us that the Hopf bifurcation when $\tau = \tau_0^-$ is subcritical, and the periodic solutions born from this first Hopf bifurcation are orbitally asymptotically stable.

Example 2. Let us now examine the second Hopf bifurcation, i.e., when $\tau^* = \tau_1^+$. Following the order of computing quantities from Example 1, this time, we obtain

$$c_1(0) \approx -0.0092 - 0.0584i.$$

Again, we have $\operatorname{Re}\{c_1(0)\}$ negative. So, the Floquet exponent β_2 is also negative. However, since $\operatorname{Re}\{\lambda'(\tau_1^+)\} > 0$ from the equation (72), we see that μ_2 from the equation (69) is positive. That is, from Theorem 2.1 and since

$$\mu_2 > 0 \qquad \text{and} \qquad \beta_2 < 0,$$

the second Hopf bifurcation when $\tau^* = \tau_1^+$ is supercritical. Moreover, the bifurcating limit-cycle solutions from this second Hopf bifurcation are orbitally asymptotically stable.

3 Numerical Simulations

In this section, we utilize a numerical continuation and bifurcation analysis tool that is suitable for the class of DDEs such as that of the system (1). Particularly, we make use of DDE-BIFTOOL [8, 9] in computing branches of equilibria and periodic solutions, and their stability, as well as numerically detecting codimension-one and codimension-two bifurcations. The latest version of this numerical package is maintained by Jan Sieber [16] and a tutorial is also available in [4].

3.1 Branches of Period-One Limit Cycles

Figure 1 shows a branch of coexistence equilibria where the age of maturation parameter τ is varied. The part of this branch in green means that E_* is LAS, while those parts in magenta mean that E_* is unstable. The points on the branch marked with $(*)$ are the points where Hopf bifurcations occur. The first Hopf bifurcation is at $\tau = \tau_0^- \approx 1.0515$, while the second Hopf bifurcation is at $\tau = \tau_1^+ \approx 2.4002$.

We can actually follow the Hopf bifurcations via DDE-BIFTOOL to obtain the branches of periodic solutions born from these Hopf bifurcations. Figure 1 also shows these branches, as well as their stability. These numerical simulations corroborate the theoretical results in the previous section. In particular, we showed in Example 1 that the first Hopf bifurcation is subcritical, and the bifurcating branch of limit cycles is orbitally asymptotically stable. In contrast, as we have shown in Example 2, the second Hopf bifurcation is supercritical, and the branch of periodic solutions emanating from this Hopf bifurcation is orbitally asymptotically stable.

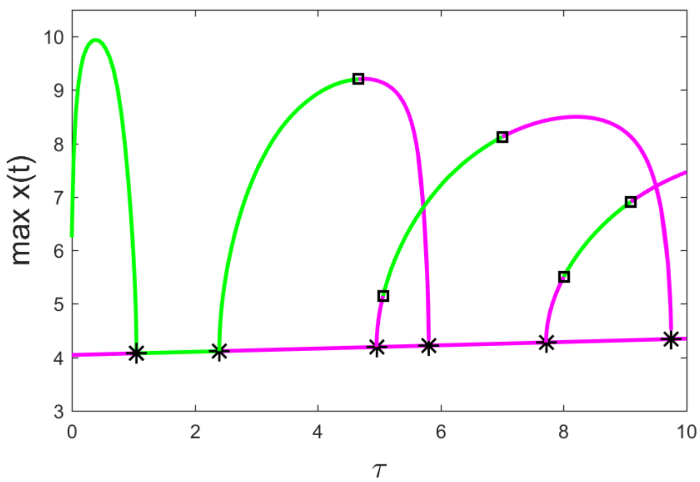

Figure 1: Branches of limit cycles emerging from the Hopf bifurcations marked with ($*$). Switches in stability along these limit-cycle branches occur at torus bifurcations marked with ($\square$). Green (resp., magenta) represents an orbitally asymptotically stable (resp., unstable) limit cycle. The same color scheme is also used for the branch of equilibria where stability switches occur at the first two Hopf bifurcations.

3.2 Quasi-Periodic Oscillations

The second, third and fourth branches of periodic solutions in Figure 1, unlike the first branch, undergo stability switches at points marked with ($\square$). These points correspond to torus bifurcations, which give rise to quasi-periodic oscillations like the one shown in Figure 3.

In Figure 2, we zoom into the portion where the second and third branches of periodic solutions overlap. Notice that at $\tau = 5$, neither the coexistence equilibrium nor the two limit cycles are stable. Apparently, in this case, one gets quasi-periodic oscillations due to the presence of the torus bifurcations, which were earlier detected using DDE-BIFTOOL. This situation means that the species still coexist while their populations undergo a rather irregular fluctuation, as illustrated in Figure 3. Previous works on the system (1), such as in [6], only showed period-one oscillations. Understanding fluctuations in species populations is indispensable in ecological studies, particularly in conservation, since recurrent low-density episodes may increase the vulnerability of populations even when all species persist.

We now provide a mechanistic interpretation of why quasi-periodic oscillations arise for large values of the time delay τ. At any given time t, the populations are shaped by the current ecological state through the immediate interaction terms in the model, that is, resource consumption, predation, and competition all depend on the densities at time t. At the same time, the mature IG-prey population at time t also depends on individuals that were produced at time $t - \tau$ and survived to maturity. This is captured by the term $b_1 e^{-\mu\tau} x(t-\tau) y(t-\tau)$. Thus, the system is influenced not only by what is happening now,

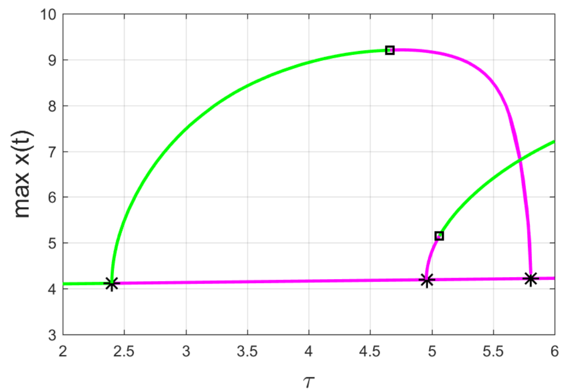

Figure 2: At $\tau = 5$, neither the coexistence equilibrium nor the limit cycles are stable.

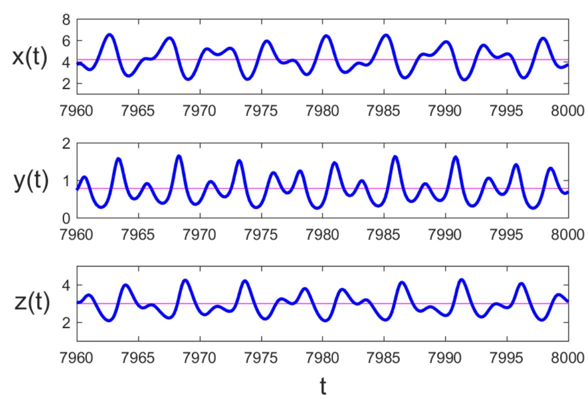

Figure 3: Quasi-periodic oscillations obtained when $\tau = 5$, where species populations follow an irregular fluctuation.

but also by conditions from τ units in the past. When τ is negligible, those two influences are still closely aligned in the sense that individuals entering the mature class were produced under ecological conditions that are not too different from the current ones. In this case, the system may still settle into a periodic rhythm. However, when τ is large, the mature recruits entering at time t may have been produced under very different conditions from those currently experienced by the populations. For instance, they may come from a time when resources were more abundant or predator pressure was weaker. As a result, the influx into the mature class may be out of phase with the present ecological state of the system. This mismatch gives a natural biological interpretation of the observed quasi-periodic oscillations. The populations are being influenced by present interactions and by delayed recruitment shaped by past conditions. If these two influences do not synchronize into one common repeating pattern, then the dynamics need not be exactly periodic. Instead, the trajectory can evolve on a torus producing the quasi-periodic solutions observed numerically.

3.3 Branches of Hopf and Torus Bifurcations

We end our numerical exploration by looking at a codimension-two bifurcation diagram. Figure 4 shows the branches of Hopf bifurcations (in blue) and the branches of torus bifurcations (in orange) in the two-parameter space. These curves were plotted on the (τ, μ)-plane, and the coexistence equilibrium E_* is LAS when the values of τ and μ are chosen inside the gray shaded region. Notice that some of the Hopf curves intersect at points marked with $(\diamond)$. These are double-Hopf bifurcations. It is well-known that, generically, branches of torus bifurcations emanate from these double-Hopf bifurcations [5, 17]. Indeed, we obtained two branches of torus bifurcations in each double-Hopf bifurcation point in Figure 4.

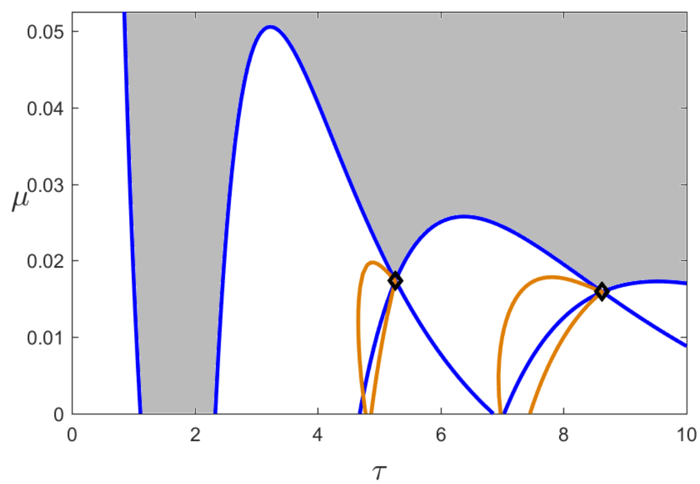

Figure 4: Branches of Hopf bifurcations (blue) and branches of torus bifurcations (orange) on the (τ, μ)-plane. Double-Hopf bifurcations are marked with $(\diamond)$. The coexistence equilibrium E_* is LAS when the values of τ and μ are chosen inside the gray shaded region.

Recall that τ is the parameter representing the maturation age in the IG prey population, while μ is the death rate of the immature IG preys. For lower values of τ, the system (1) can only exhibit period-one oscillations. However, for larger values of τ, more complex dynamics may arise, including quasi-periodic oscillations which are attributed to the presence of double-Hopf and torus bifurcations.

Another interesting interpretation coming from the two-parameter bifurcation diagram in Figure 4 is through the first Hopf curve where τ is between 0 and 2. Here, the coexistence equilibrium is LAS when the values of τ and μ are chosen to the right of this curve. When the death rate μ is high, i.e., when the species is threatened, the value of the maturation age τ should be lower in order for the coexistence equilibrium E_* to be LAS. This observation has some implications on conservation efforts and ecological management, e.g., looking at species' age of maturation as an indicator of its vulnerability [11].

4 Summary and Conclusions

In this work, we revisited the three-species intraguild predation model that was shown previously to undergo Hopf bifurcations around the coexistence equilibrium. Building on this earlier work, we determined the criticality or the direction of the Hopf bifurcations, as well as the stability of the limit cycles born from these Hopf bifurcations. The main tool in deriving the main results is the centre manifold reduction and the normal form theory that applies to our model, which is a system of delay differential equations with delay-dependent parameters. Our numerical simulations corroborate the theoretical results, and also lead to the discovery of codimension-two bifurcations, such as double-Hopf and torus bifurcations. The presence of these bifurcations justifies the observed quasi-periodic oscillations for certain values of the age-of-maturation parameter when neither the coexistence equilibrium nor the period-one limit cycle is stable. The study also has some implications on conservation efforts and ecological management, e.g., looking at species' age of maturation as an indicator of its vulnerability.

Acknowledgments

The authors are grateful to the referees for their valuable review that greatly improved the quality of this paper. The authors also acknowledge the support of the University of the Philippines Baguio.

References

[1] M. Ait Babram, An algorithmic scheme for approximating center manifolds and normal forms for functional differential equations, in: O. Arino, M.L. Hbid, E. Ait Dads (Eds.), *Delay Differential Equations and Applications*, Springer, Dordrecht, 2006, pp. 193–226.

[2] L. Barreira, C. Valls, *Center manifolds for delay equations*, Funkcial. Ekvac. **63** (2020) 39–65.

[3] E. Beretta, Y. Kuang, *Geometric stability switch criteria in delay differential systems with delay dependent parameters*, SIAM J. Math. Anal. **33** (2002) 1144–1165.

[4] J.A. Collera, Numerical continuation and bifurcation analysis in a harvested predator-prey model with time delay using DDE-Biftool, in: M. Mohd, N. Abdul Rahman, N. Abd Hamid, Y. Mohd Yatim (Eds.), *Dynamical Systems, Bifurcation Analysis and Applications*, Springer, Singapore, 2019, pp. 225–241.

[5] J.A. Collera, *Bubbling, bistable limit cycles and quasi-periodic oscillations in queues with delayed information*, Symmetry **14** (2022) 376.

[6] J.A. Collera, F.M.G. Magpantay, Dynamics of a stage structured intraguild predation model, in: D. Kilgour, H. Kunze, R. Makarov, R. Melnik, X. Wang (Eds.), *Recent*

Advances in Mathematical and Statistical Methods, Springer, Cham, 2018, pp. 327–337.

[7] O. Diekmann, S.A. van Gils, The center manifold for delay equations in the light of suns and stars, in: M. Roberts, I. Stewart (Eds.), *Singularity Theory and its Applications*, Springer, Berlin, Heidelberg, 1991, pp. 122–141.

[8] K. Engelborghs, T. Luzyanina, D. Roose, *Numerical bifurcation analysis of delay differential equations*, J. Comput. Appl. Math. **125** (2000) 265–275.

[9] K. Engelborghs, T. Luzyanina, D. Roose, *Numerical bifurcation analysis of delay differential equations using DDE-BIFTOOL*, ACM Trans. Math. Softw. **28** (2002) 1–21.

[10] T. Faria, Normal forms and bifurcations for delay differential equations, in: O. Arino, M.L. Hbid, E. Ait Dads (Eds.), *Delay Differential Equations and Applications*, Springer, Dordrecht, 2006, pp. 227–282.

[11] J.L. Gosselin, B.P. Sandford, C.S. O'Brien, E.R. Buhle, *Biological, freshwater, and marine drivers of age at maturity in wild Chinook Salmon*, bioRxiv (December 2025), DOI: 10.64898/2025.12.13.694134

[12] S. Guo, J. Wu, *Bifurcation Theory of Functional Differential Equations*, Springer, New York, 2013.

[13] J.K. Hale, S.M. Verduyn Lunel, *Introduction to Functional Differential Equations*, Springer-Verlag, New York, 1993.

[14] B.D. Hassard, N.D. Kazarinoff, Y.H. Wan, *Theory and Applications of Hopf Bifurcation*, Cambridge University Press, Cambridge, 1981.

[15] R.D. Holt, G.A. Polis, *A theoretical framework for intraguild predation*, Am. Nat. **149** (1997) 745–764.

[16] T. Luzyanina, J. Sieber, K. Engelborghs, G. Samaey, D. Roose, *Numerical bifurcation analysis of mathematical models with time delays with the package DDE-BIFTOOL*, Mat. Biolog. Bioinform. **12** (2017) 496–520.

[17] N.F. Tehrani, M. Razvan, *Bifurcation structure of two coupled FHN neurons with delay*, Math. Biosci. **270** (2015) 41–56.

[18] Y. Wang, J. Wu, Y. Xiao, *A stage structured predator-prey model with time delays*, Rocky Mt. J. Math. **38** (2008) 1721–1743.

[19] M. Yamaguchi, Y. Takeuchi, W. Ma, *Dynamical properties of a stage structured three-species model with intra-guild predation*, J. Comput. Appl. Math. **201** (2007) 327–338.

This page is intentionally left blank